DP-1485



# EXOTHERMIC REACTIONS LEADING TO UNEXPECTED MELTDOWN OF SCRAP URANIUM-ALUMINUM CERMET CORES DURING OUTGASSING

L. W. GRAY
W. J. KERRIGAN

---

E. I. DU PONT DE NEMOURS AND COMPANY
SAVANNAH RIVER LABORATORY
AIKEN, SOUTH CAROLINA 29801

PREPARED FOR THE U.S. DEPARTMENT OF ENERGY UNDER CONTRACT AT(07-2)-1

Printed in the United States of America

Available from
National Technical Information Service
U.S. Department of Commerce
5285 Port Royal Road
Springfield, Virginia 22161

Price: Printed Copy $4.50; Microfiche $3.00

662751

DP-1485
Distribution Category UC-4

# EXOTHERMIC REACTIONS LEADING TO UNEXPECTED MELTDOWN OF SCRAP URANIUM-ALUMINUM CERMET CORES DURING OUTGASSING

by

L. W. Gray
W. J. Kerrigan

Approved by

R. L. Folger
Analytical Chemistry Division
Savannah River Laboratory

Publication Date: March 1978

---

E. I. DU PONT DE NEMOURS AND COMPANY
SAVANNAH RIVER LABORATORY
AIKEN, SOUTH CAROLINA 29801

PREPARED FOR THE U.S. DEPARTMENT OF ENERGY UNDER CONTRACT AT(07-2)-1

## ABSTRACT

During routine outgassing of scrap uranium-aluminum cermet cores, unexpected exothermic reactions released sufficient energy to melt nine cores. In the subsequent investigation, compounds in the scrap uranium were identified, the history of the material was defined, and thermal analysis studies were made. The incident was initiated by reactions at ∿350°C between powdered aluminum metal and sodium uranate salt, $Na_2U_2O_7$. These reactions released sufficient energy to initiate aluminothermic reduction of $(NH_4)_3UO_2F_5$, $NaNO_3$, $UO_3$, and $U_3O_8$. The energy release from aluminothermic reduction reactions was sufficient to melt the cermet cores.

## CONTENTS

## LIST OF FIGURES



## LIST OF TABLES

# EXOTHERMIC REACTIONS LEADING TO UNEXPECTED MELTDOWN OF SCRAP URANIUM-ALUMINUM CERMET CORES DURING OUTGASSING

## INTRODUCTION

The Savannah River Plant (SRP) regularly receives spent fuel and scrap powders containing uranium, neptunium, plutonium, and other actinides from U. S. Department of Energy (DOE) and Department of Defense (DOD) sites. Upon receipt, these materials are modified by physical, chemical, or metallurgical techniques[1-4] to render them compatible with the solvent extraction processes in use at SRP. Enriched uranium and neptunium are recovered by the "Uranium-235" (HM) process[5-8] and plutonium is recovered by the Purex process.[5,9,10]

This report presents the pertinent facts leading up to the unexpected meltdown of cermet cores of powdered aluminum metal and scrap uranium during routine outgassing, an analysis of the cause of the exothermic reactions, and the methods used to recover the uranium contained within the reactive billets.

## RESULTS OF ANALYSES

Scrap enriched uranium, labeled as uranium oxide, was received from two offplant sites for recovery of uranium. The material, received in 101 separate containers, was blended with aluminum powder, and weighed amounts were compacted to about 80% of theoretical density (TD). These individual compacts were then loaded into aluminum housings and welded to form 74 extrusion billets. Thirty-two billets were successfully outgassed and extruded into tubes, and the uranium was recovered by the HM production process without incident. During routine outgassing of 35 additional billets, violent exothermic reactions occurred which partially or completely melted 9 of the billet cores. These 35 billets plus the remaining 7 billets were stored pending an investigation of the causes of meltdown.

Subsequent analysis showed that 28 of the remaining 42 billets did not contain reactive materials. Twenty-seven of these 28 billets were processed routinely via outgassing, extrusion, and dissolution. The 28th billet became contaminated during storage and handling and was set aside for special processing along with the 14 billets containing reactive materials.

Of the remaining 14 billets containing reactive or potentially reactive materials, the 9 billets which partially or completely melted were shown to contain varying amounts of sodium uranate, $Na_2U_2O_7$, which reacts exothermically with powdered aluminum metal at ~350°C. This reaction releases sufficient energy to initiate aluminothermic reduction of $(NH_4)_3UO_2F_5$, $NaNO_3$, $UO_3$, and $U_3O_8$. The 5 billets which showed no visible external signs of reaction were shown to contain varying amounts of $(NH_4)_3UO_2F_5$, $U_3O_8$, and $UO_3$. Recovery of uranium by reduction to form an aluminum-uranium alloy, followed by dissolution of the alloy, was successfully demonstrated with 4 of the reactive billets.

## CONCLUSIONS

The initial reaction of importance in each of the melted cores was the solid-state reaction: $3Na_2U_2O_7 + 4\ Al \rightarrow 3Na_2O + 2Al_2O_3 + 6UO_2$. Although this reaction occurs only at the particle boundaries of the reacting powders, sufficient heat was generated to initiate the reactions between sodium nitrate and $(NH_4)_3UO_2F_5$ with aluminum. These two reactions accounted for about 93% of the total heat evolved during the meltdown incident. Sufficient energy was released during these reactions to initiate the reduction by aluminum of $U_3O_8$, $UO_3$, and other impurities such as $Fe_2O_3$.

The incident was the result of a series of operating errors:

A. Sodium hydroxide instead of ammonium hydroxide was used to precipitate $UO_2^{2+}$ from nitric acid pickling solutions.

B. Sodium nitrate occluded in the mixed uranate ($Na_2U_2O_7$-$Na_6U_7O_{24}$) precipitate was not washed from the product.

C. The precipitates from the pickling solutions and from an ion exchange process were calcined at a temperature less than 500°C, probably as low as 350°C. If the products had been calcined at 600°C, both the sodium nitrate and $(NH_4)_3UO_2F_5$ would have decomposed.

D. These materials were labeled as scrap uranium oxide, even though the shipper knew they were not uranium oxide, and his analytical reports showed the presence of uranium compounds other than uranium oxide.

E. There was insufficient test screening of the scrap material at SRP.

F. The significance of the different chemical compositions reported by the shipper and the fact that the shipper's analyses accounted for less than 50% of the material was not recognized at SRP.

## RECOMMENDATIONS

It is recommended that all scrap material be chemically characterized. Process conditions should then be simulated before large amounts of scrap are submitted for recovery. To aid in this characterization, all scrap sent to another site for recovery should be accompanied with a document containing the following items:

1. Stable-element and radionuclide analyses of the product shipped, including impurities. Total analysis should add up to 100 ±5%.

2. A history of the material, including the following items:

   (a) Point of origin — pickling-bath solution, slag and crucible from bomb reduction, etc.

   (b) Chemical additions to convert from original material to product shipped.

   (c) Drying and/or calcining conditions — temperature, time, atmosphere, batch size.

   (d) Storage conditions — dry, humid, radioactive, oxidizing, reducing, air or inert atmosphere, under liquid, etc.

   (e) Fabrication conditions — hot-pressed, cast, machined — along with atmosphere and temperature.

## DESCRIPTION OF INCIDENT

Enriched uranium from scrap oxide powders from other sites is recovered at SRP. A powder metallurgical technique which encapsulates the scrap oxide in aluminum cermet cores for extrusion into aluminum-clad tubes (to provide safe processing from a nuclear criticality standpoint) was chosen to prepare a large quantity of material for dissolution and subsequent recovery as $^{235}UO_2(NO_3)_2$ solution.

Upon receipt of the first two shipments of the scrap, random samples were analyzed chemically for uranium and were subjected to differential thermal analysis (DTA). Neither the chemical and emission spectroscopic data from the shipper, nor the analyses of the as-received powders at SRP gave any indication of potential problems.

Upon completion of these analyses, a pilot test of 4 cermet cores was prepared as follows: the scrap oxide powder was ball-milled, screened (-40 mesh), blended with aluminum powder Type 101 (-100 to +200 mesh, 0 to 5%; -200 to -325 mesh, 10 to 25%; -325 mesh, 75 to 90%), and compacted to about 80% of theoretical density. These individual compacts were then loaded into aluminum housings and welded to form extrusion billets. The billets were outgassed by slowly heating them to 525°C, evacuated to remove air and volatile materials, and sealed under vacuum. Upon extrusion, the core density increased to >99% of theoretical. Ring samples were cut from one tube for dissolution tests.

Based on these successful pilot tests, an additional 28 billets were prepared from powders received in the first two shipments and extruded. The 32 tubes were then routinely processed by loading into bundles, lowering into critically safe dissolver inserts, and dissolving. The $^{235}U$ was recovered by the "Uranium-235" process without incident.

A third shipment of scrap powder of slightly different chemical composition was used to prepare a group of 42 cermet billets in the same manner as the previous batches; the significance of the slightly different chemical composition was not recognized prior to billet preparation. The routine outgassing operation consisted of placing several billets in the steel catchpans of an outgassing furnace, raising the temperature to 250°C for 40 minutes, and performing a leak rate test to assure that the billets were free of holes and that the vacuum system was not plugged. The furnace temperature was raised to the outgassing temperature of 525°C while billets were being evacuated. The outgassing continued for ∿24 hours before the furnace was cooled and each billet sealed.

During the outgassing of 11 billets from this third shipment of scrap powder, the outgassing operation proceeded normally through the leak-checking step. Heating was continued to bring the billets to the outgassing temperature of 525°C. When the temperature reached 345°C, a violent, exothermic reaction occurred in 6 of the billet cores, with a calculated release of 10,000 to 60,000 kilocalories of energy. Figure 1 is a temperature trace of the furnace during this incident; Figure 2 shows different views of the reacted cores. The reaction was totally contained, preventing release of radioactive material. There were no injuries or significant equipment damage, and there would have been no criticality problem even if the steel catchpans had melted. Subsequent examination showed that 9 of 35 billets that were outgassed in three furnaces exhibited exothermic core reactions. Processing of the 35 billets was deferred, and the remaining 7 billets of this group were stored pending an investigation of the causes of the meltdown.

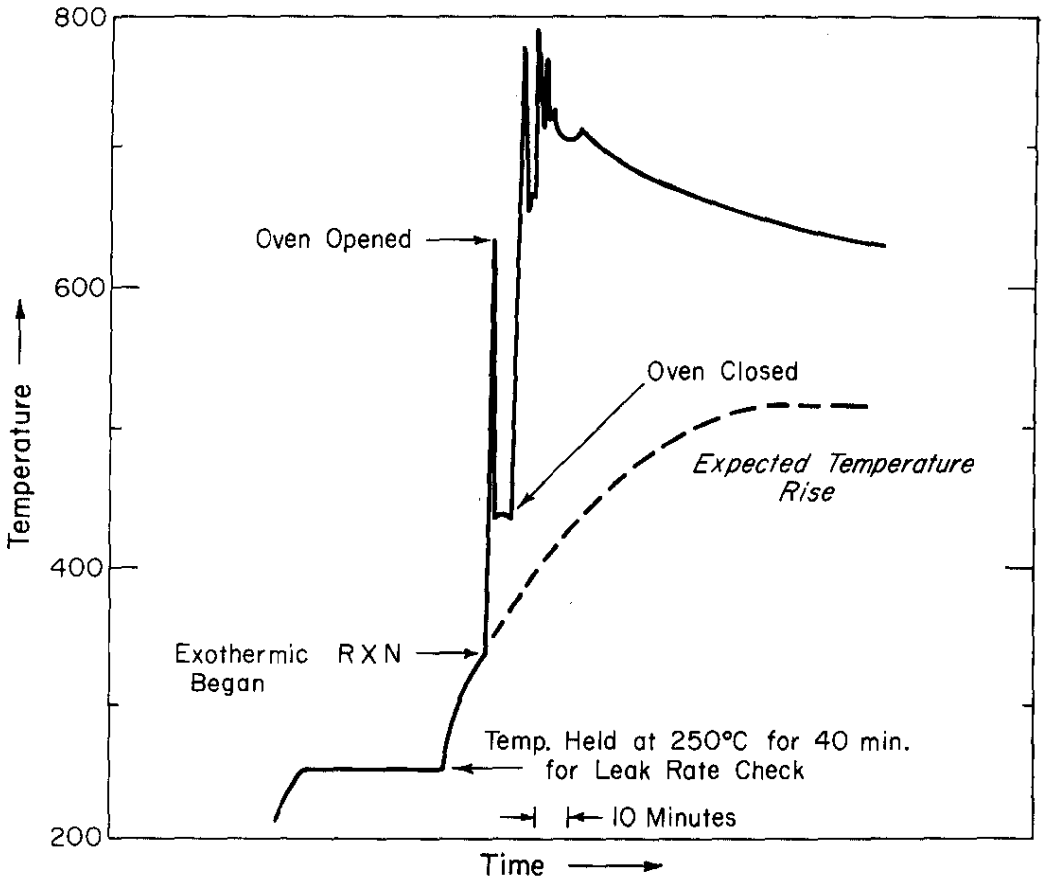


FIGURE 1. Temperature Trace of Furnace "B" 6/2/72

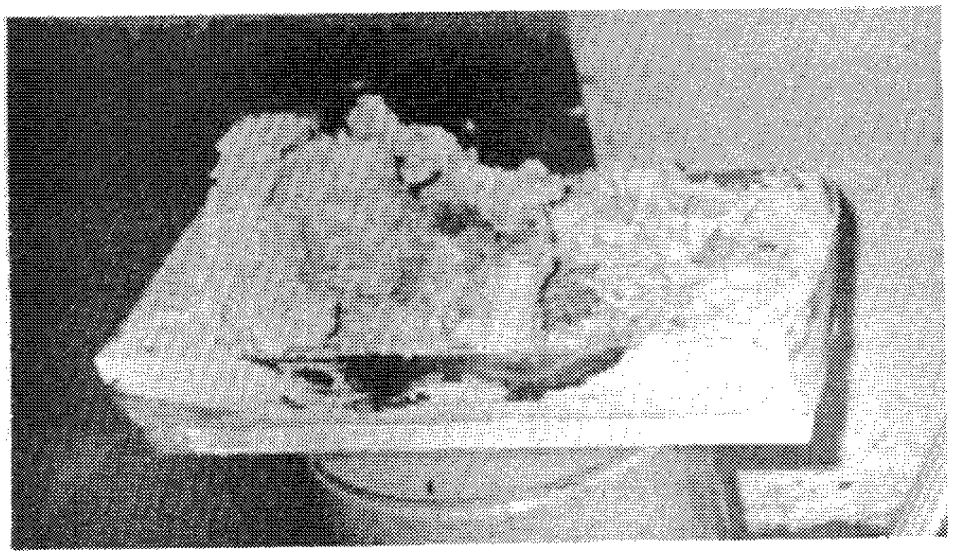

a. Side View

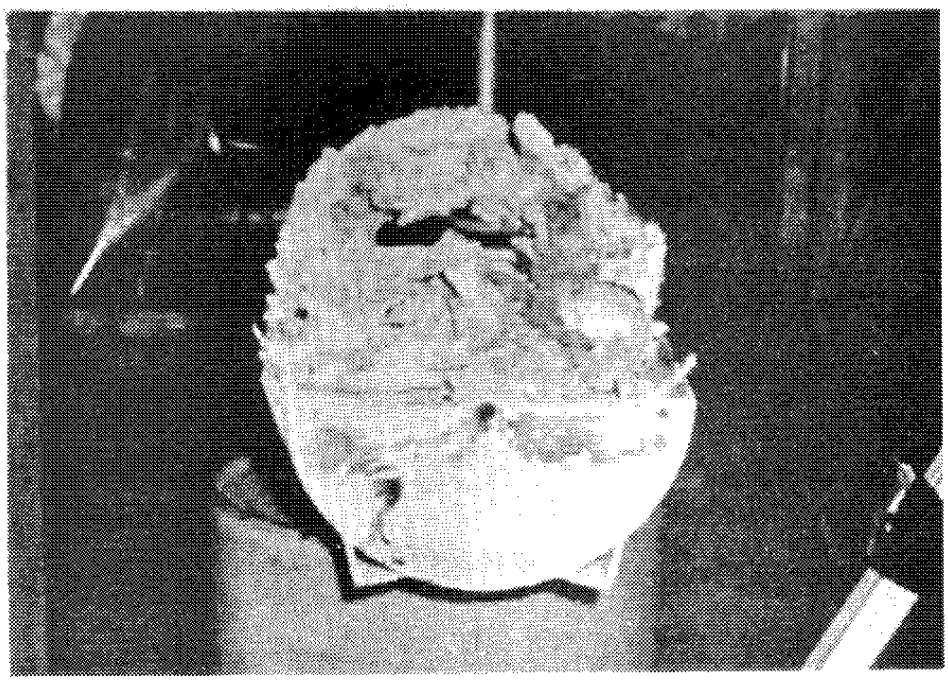

b. End View

FIGURE 2. Reacted Cores

## INVESTIGATION

### Elemental and Compound Analysis of Scrap Materials

As a result of the unexpected, violent, exothermic reactions a program was undertaken to (a) identify the elements or compounds which caused the reactions, and (b) develop and define a recovery method for the remaining 42 enriched uranium-aluminum billets.

Elements and compounds in samples of the original scrap oxide powders were identified by combinations of the following methods: spark source mass spectrometry (SSMS); atomic absorption (AA) and flame emission spectroscopy; elemental analysis for C, H, N and O; ion-selective electrode measurements; x-ray diffraction; infrared and Raman spectroscopy; and alpha pulse height and chemical analysis. Based on these analyses, four different groups of scrap oxide powders were identified. Results are listed in Table 1. A complete elemental analysis is given for Group D materials in Table 2.

### History of Scrap Uranium

A total of 101 containers reported to contain scrap $^{235}U_3O_8$ was received from two offsite locations. The material had been produced over a period of 6 to 8 years, and the history of the material was not readily available. The 101 containers of material were divided into four groups (A,B,C, and D) according to their compositions, as noted above, and also according to their thermal behavior. Billets that exhibited exothermic core reactions contained scrap oxide from Groups C and D. Intersite discussions based on these data led to a reasonable narrative of the source and history of the scrap materials.

Group A materials came mainly from nitric acid pickling baths. The nitric acid solutions were concentrated by evaporation in stainless steel evaporators, and the bottoms were precipitated by the addition of aqueous ammonia. The resulting ammonium diuranate (ADU) was then calcined at about 300 to 450°C to form the orange-colored $\beta$-$UO_3$. This material was contaminated with evenly dispersed stainless-steel corrosion products, borosilicate glass, and what appeared to be a montmorillonite clay [an additive to *Met-L-X* (Ansul Chemical Co., Marinette, Wisconsin), a common fire-extinguishing agent for metal fires].

TABLE 1

Compounds Identified in the Scrap Oxide Powders

| *Group A* | | *Group B* | | *Group C* | | *Group D* | |
|---|---|---|---|---|---|---|---|
| *Compounds* | *(% Avg)* | *Compounds* | *(% Avg)* | *Compounds* | *%* | *Compounds* | *%* |
| $UO_3$ | 80 | Subgroup 1 | | $(NH_4)_3UO_2F_5$—$U_3O_8$ | 70 | $(Na,K)_2U_2O_7$—$(Na,K)_6U_7O_{24}$ | 23 |
| $H_2O$ | 0.5 | $U_3O_8$ | 97 | $AlF_3$-$Al_2O_3$ | 30 | $(Na,K)NO_3$ | 36 |
| Clay | ∿5 | $H_2O$ | 0.4 | | | $(Cd,Pb,Cu)CO_3$—$(Na,K)HCO_3$ | 16 |
| $(Fe,Cr)_2O_3$ | ∿10 | $(Fe,Cr)_2O_3$ | 2.5 | | | $(Fe,Cr)_2O_3$ | 7 |
| NiO | 0.7 | | | | | NiO | 0.2 |
| Glass | ∿4 | Subgroup 2 | | | | $Co_3O_4$ | 0.1 |
| | | $U_3O_8$ | >98 | | | $(Na,K,Li)HSO_4$ | 5 |
| | | $H_2O$ | ∿0.2 | | | $(Na,K,Li)H_2PO_4$ | 5 |
| | | $(Fe,Cr)_2O_3$ | <1 | | | $(Na,K,Li)(F,Cl)$ | 6 |
| | | Subgroup 3 | | | | $H_2O$ | 0.2 |
| | | $U_3O_8$ | 83 | | | | |
| | | $(Fe,Cr)_2O_3$ | 14 | | | | |
| | | NiO | 0.5 | | | | |
| | | $Co_3O_4$ | 0.2 | | | | |
| | | $(NaK,M)_xH_yPO_4$ | ∿3 | | | | |
| | | M = Ca, etc. | | | | | |

TABLE 2

Analyses of Group D Materials

| | *Concentration, wt %* | | | | | | | | | |
|---|---|---|---|---|---|---|---|---|---|---|
| Container 6M — | 013 | 019 | 035 | 089 | 143 | 145 | 176 | 281 | 305 | Avg. |
| *Element or Compound* | | | | | | | | | | |
| U | 18.8 | 18.8 | 14.5 | 13.8 | 16.7 | 14.0 | 14.5 | 14.0 | 18.8 | 16.0 |
| O | 46.0 | 45.7 | 45.4 | 44.3 | 44.1 | 44.5 | 44.0 | 44.5 | 42.0 | 44.5 |
| Na | 11.86 | 9.67 | 11.71 | 12.57 | 11.22 | 12.24 | 12.70 | 13.19 | 13.90 | 12.12 |
| K | 4.77 | 4.65 | 5.58 | 3.90 | 4.25 | 5.26 | 5.48 | 5.60 | 4.71 | 4.91 |
| N | 5.9 | 5.8 | 5.9 | 6.0 | 6.1 | 6.0 | 5.8 | 5.8 | 6.0 | 5.92 |
| Fe | 2.76 | 2.95 | 2.85 | 2.60 | 2.91 | 2.70 | 2.43 | 2.83 | 3.04 | 2.79 |
| C | 0.86 | 1.7 | 0.71 | 0.99 | 1.08 | 0.93 | 1.11 | 1.16 | 1.27 | 1.09 |
| H | 1.00 | 1.00 | 0.79 | 0.90 | 0.51 | 1.25 | 0.95 | 0.97 | 1.00 | 0.93 |
| Cr | 0.78 | 0.84 | 0.81 | 0.69 | 0.79 | 0.77 | 0.74 | 0.80 | 0.84 | 0.78 |
| Cd | 0.54 | 0.62 | 0.94 | 0.58 | 0.55 | 0.59 | 0.65 | 0.62 | 0.70 | 0.61 |
| Pb | 0.10 | 0.10 | 0.08 | 0.09 | 0.09 | 0.08 | 0.08 | 0.09 | 0.10 | 0.09 |
| Ca | 0.41 | 0.35 | 0.55 | 0.22 | 0.24 | 0.50 | 0.31 | 0.41 | 0.21 | 0.36 |
| Ni | 0.18 | 0.21 | 0.022 | 0.17 | 0.17 | 0.17 | 0.15 | 0.19 | 0.22 | 0.19 |
| Li | 0.48 | 0.46 | 0.46 | 0.36 | 0.38 | 0.42 | 0.35 | 0.45 | 0.38 | 0.41 |
| Co | 0.006 | 0.007 | 0.007 | 0.006 | 0.006 | 0.006 | 0.006 | 0.007 | 0.008 | 0.007 |
| S | 1.30 | 1.32 | 1.33 | 1.37 | 1.40 | 1.31 | 1.35 | 1.34 | 1.36 | 1.34 |
| P | 1.30 | 1.28 | 1.27 | 1.40 | 1.20 | 1.30 | 1.28 | 1.29 | 1.30 | 1.29 |
| Cl | 2.40 | 2.41 | 2.45 | 2.48 | 2.38 | 2.44 | 2.43 | 2.45 | 2.43 | 2.43 |
| F | 0.08 | 0.88 | 0.85 | 0.82 | 0.92 | 0.88 | 0.86 | 0.89 | 0.86 | 0.87 |
| $H_2O$ | 0.20 | 0.30 | 0.15 | 0.11 | 0.25 | 1.04 | 0.24 | 0.23 | 0.29 | 0.31 |
| Total | 100.51 | 99.05 | 96.20 | 93.36 | 95.25 | 96.39 | 95.42 | 96.82 | 99.42 | 96.95 |

Subgroups 1 and 3 of Group B materials (Table 1) were recovered from nitric acid pickling baths. These materials were concentrated and precipitated similar to the Group A materials. The resulting ADU was calcined at about 600°C to form $\alpha$-$U_3O_8$. The stainless steel corrosion products in this material fell into two fairly uniform groups, indicating at least two different pickling bath cleanup campaigns. Subgroup 2 materials (Table 1) were from a different offplant site. The history of this material was not traced.

Group C materials were obtained from an ion-exchange separation of neptunium and uranium. In this process, $Al^{3+}$ ion was used as a masking agent for fluoride ion. After separation, the resulting solution contained aluminum and uranium ions in mixed nitric-hydrofluoric acids. This acidic solution was concentrated by evaporation, and aqueous ammonia was added. The resulting precipitate was incompletely calcined at <600°C. The calcined products were mixtures of $Al_2O_3$, $AlF_3$, $(NH_4)_3UO_2F_5$, and $U_3O_8$.

Group D materials were also recovered from nitric acid pickling baths. These solutions were concentrated by evaporation, and the uranium salts were precipitated by the addition of a mixture of sodium and potassium hydroxides. The precipitate was calcined at less than 600°C (probably at 350°C) to form a mixture of $(Na,K)_2U_2O_7$, $(Na,K)_6U_7O_{24}$, $(Na,K)NO_3$, and a number of other minor products.

## Blending of Scrap Material

In the recovery process, the scrap uranium powders were blended to keep weight loss less than a defined maximum value after ignition to 500°C. Each charge was then blended with aluminum powder to meet specified aluminum metal/scrap powder ratios. Weighed amounts were compacted to about 80% of theoretical density and these individual compacts were loaded into aluminum housings and welded to form extrusion billets. From the blending data, the composition of each blend (and therefore each individual compact and each billet) was determined. Each billet, however, contained 48 compacts which were prepared from two or more blends of scrap uranium and aluminum powders. The composite analyses of the scrap powder in each billet is given in Table 3. For the 14 billets which were subsequently set aside for special processing, the blending data are given in Table 4.

## Thermal Analysis of Scrap Material

Most of the DTA data were obtained either with 25.0 mg of powder or 25 ±0.5 mg of broken fragments from a compressed pellet. The instrument atmosphere was 4% $H_2$ - 96% Ar, and the heating and cooling rates were either 10°C/min or 25°C/min. DTA data from the four groups of scrap powders showed no significant exothermic events (Figures 3 through 5). The powders did show a number of reversible and nonreversible endothermic reactions over the temperature range of ambient to 1100°C in the $H_2$-Ar atmosphere. However, when the scrap powders were blended with aluminum powder, compacted to about 80% of theoretical density, and then subjected to DTA, pronounced differences in the four groups were evident.

TABLE 3

Composition of Extrusion Billets

| | *Component of Scrap Powder, wt %* | | | |
|---|---|---|---|---|
| *Billet* | *Group A* | *Group B* | *Group C* | *Group D* |
| 1001-1050 | | 100 | | |
| 1051 | | 40.45 | 59.55 | |
| 1052 | | 60.34 | 39.66 | |
| 1053 | | 16.78 | 74.90 | 8.31 |
| 1054 | | 32.14 | 19.93 | 47.95 |
| 1055 | | 27.87 | 22.13 | 50.00 |
| 1056 | 35.10 | | 14.90 | 50.00 |
| 1057 | 56.32 | | | 43.68 |
| 1058 | 3.77 | | 50.49 | 45.73 |
| 1059 | | | 50.00 | 50.00 |
| 1060 | | 35.96 | 31.70 | 32.34 |
| 1061 | | 23.38 | 33.74 | 42.88 |
| 1062 | 73.40 | 4.04 | 16.12 | 6.43 |
| 1063 | 89.98 | | 10.00 | |
| 1064 | 100 | | | |
| 1065 | 84.51 | | 15.49 | |
| 1066-1074 | | 100 | | |

TABLE 4

Blending Data for Billets Containing Reactive Materials

| Billet | Blend | Compacts, No. | Scrap Powder Composition, wt % Group A | Group B | Group C | Group D |
|---|---|---|---|---|---|---|
| 1051 | 5UB13A | 18 | | 100 | | |
| | 5UB13B | 18 | | | 100 | |
| | 5UB14A | 12 | | 6.12 | 93.88 | |
| 1052 | 5UB14A | 8 | | 6.12 | 93.88 | |
| | 5UB14B | 18 | | 50.40 | 49.60 | |
| | 5UB15A | 18 | | 100 | | |
| | 5UB15B | 4 | | 26.00 | 74.00 | |
| 1053 | 5UB15B | 15 | | 26.00 | 74.00 | |
| | 5UB16 | 22 | | | 100.0 | |
| | 5UB17 | 11 | | 36.75 | 26.50 | 36.75 |
| 1054 | 5UB17 | 14 | | 36.75 | 26.50 | 36.75 |
| | 5UB18 | 22 | | 45.91 | | 54.09 |
| | 5UB19 | 12 | | | 50.00 | 50.00 |
| 1055 | 5UB19 | 10 | | | 50.00 | 50.00 |
| | 5UB20 | 26 | | 50.00 | | 50.00 |
| | 5UB21 | 12 | | | 50.00 | 50.00 |
| 1056 | 5UB21 | 15 | | | 50.00 | 50.00 |
| | 5UB22 | 31 | 50.00 | | | 50.00 |
| | 5UB23 | 2 | 50.00 | | | 50.00 |
| 1057 | 5UB23 | 24 | 50.00 | | | 50.00 |
| | 5UB24 | 24 | 62.56 | | | 37.44 |
| 1058 | 5UB24 | 3 | 62.56 | | | 37.44 |
| | 5UB25 | 25 | | | 50.00 | 50.00 |
| | 5UB26 | 20 | | | 58.39 | 41.61 |
| 1059 | 5UB26 | 5 | | | 58.39 | 41.61 |
| | 5UB27 | 25 | | | 50.00 | 50.00 |
| | 5UB28 | 18 | | | 47.73 | 52.27 |
| 1060 | 5UB28 | 6 | | | 47.73 | 52.27 |
| | 5UB29 | 25 | | | 50.00 | 50.00 |
| | 5UB31 | 17 | | 100.0 | | |
| 1061 | 5UB31 | 7 | | 100 | | |
| | 5UB30 | 25 | | | 41.21 | 58.79 |
| | 5UB32 | 16 | | 23.98 | 37.90 | 38.12 |
| 1062 | 5UB32 | 9 | | 23.98 | 37.90 | 38.12 |
| | 5UB33 | 25 | 100 | | | |
| | 5UB34 | 14 | 69.42 | | 30.58 | |
| 1063 | 5UB34 | 15 | 69.42 | | 30.58 | |
| | 5UB35 | 23 | 100 | | | |
| | 5UB36 | 10 | 100 | | | |
| 1065 | 5UB38 | 23 | 60.38 | | 39.62 | |
| | 5UB39 | 25 | 100.0 | | | |

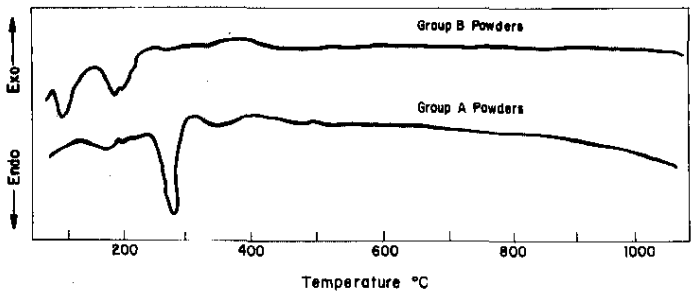


FIGURE 3. Typical DTA Curves for Groups A and B Materials

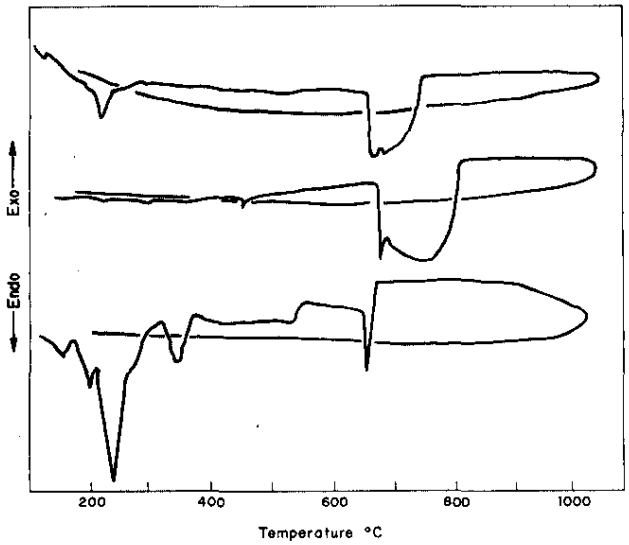


FIGURE 4. Typical DTA Curves for Group C Materials

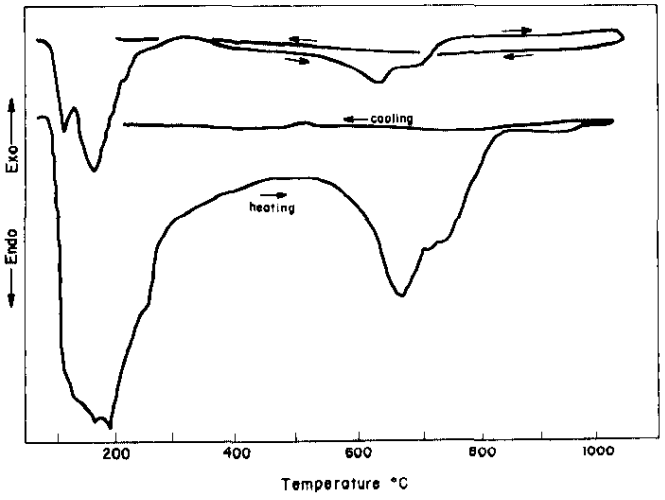


FIGURE 5. Typical DTA Curves for Group D Materials

Powders in Groups A and B exhibited exothermic solid-state reactions with aluminum powder at about 630 to 660°C (Figures 6 and 7). This reaction was slow and was apparently quenched by the melting of aluminum at 660°C. When heating was interrupted before the melting point of aluminum, and the pellets were quenched, ground and recompacted, there was additional reaction in the 630 to 660°C region. From these data, the 630 to 660°C reaction was assumed to occur only at the particle boundaries. An additional exothermic reaction was observed to begin at about 800 to 850°C.

Compacts of Group C powders underwent a large exothermic reaction beginning at about the aluminum melting point (Figure 8). As with Group A and B powders, an additional exothermic reaction was observed to begin at about 800 to 850°C.

Group D powders underwent an exothermic solid-state reaction with aluminum beginning at about 350°C (Figure 9). This reaction apparently also occurs only at the particle boundaries of the compacted powders. A second exothermic solid-state reaction began in some of the powders at about 630°C. In all cases, this exotherm was quite small and was not reproducible even in the same blend of Al-scrap powders. In those cases where it was discernible, the exothermic reaction was quenched by the melting of aluminum at 660°C. An additional exothermic reaction of the material began at about 750°C. The heat evolved from this reaction also varied from batch to batch among Group D powders.

Areas under the DTA curves were used to estimate the heat released during individual reactions (Table 5). From this table, it is evident that the exothermic reactions in the billets were initiated by Group D powders. It is further evident that the Group C powders are ignited by the low temperature exothermic reactions of Group D powders. Heat released during these reactions then ignited the high temperature exotherm of the Group D powders. It was estimated that these two reactions (Group C - Al and high-temperature Group D - Al) provided about 93% of the total energy release during the outgassing of the billets.

From the composite analyses of each billet (Table 3) and from the estimated energy releases of each type of scrap powder (Table 5), the energy available for release from low (300 to 600°C), intermediate (600 to 800°C), and high temperature (>800°C) aluminothermic reactions were derived for each billet. Results of these calculations are shown in Table 6.

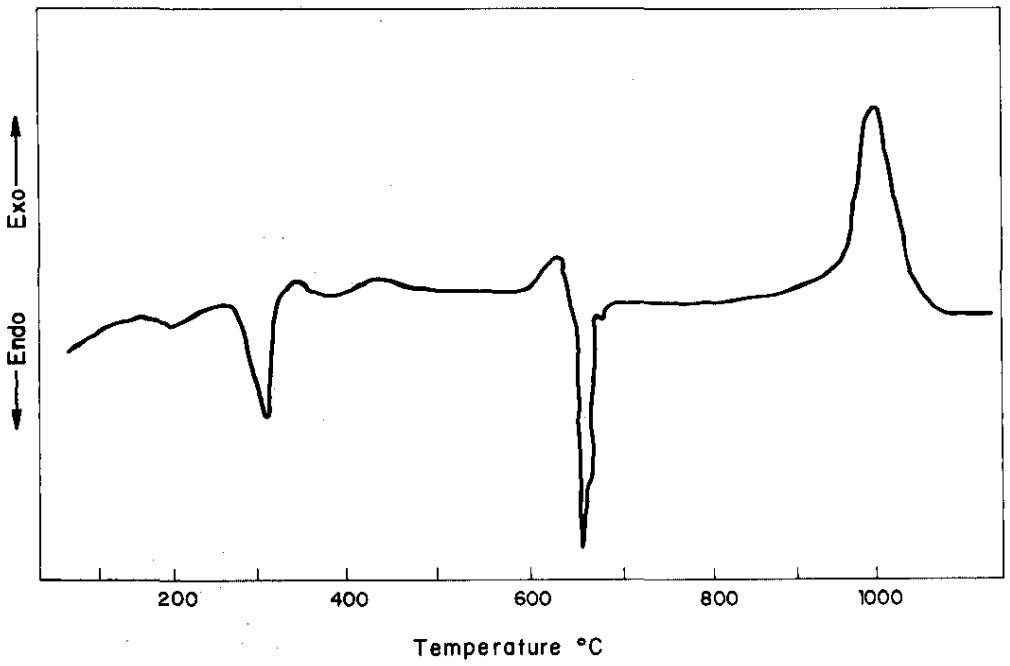


FIGURE 6. Typical DTA Curve for Group A-Al Compact

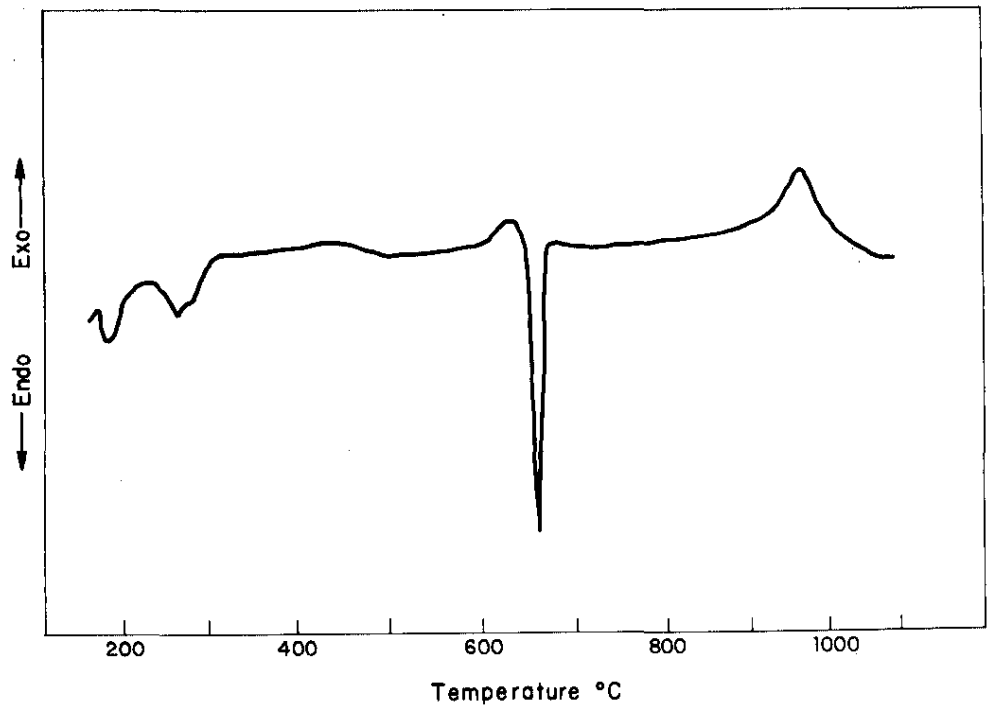


FIGURE 7. Typical DTA Curve for Group B-Al Compact

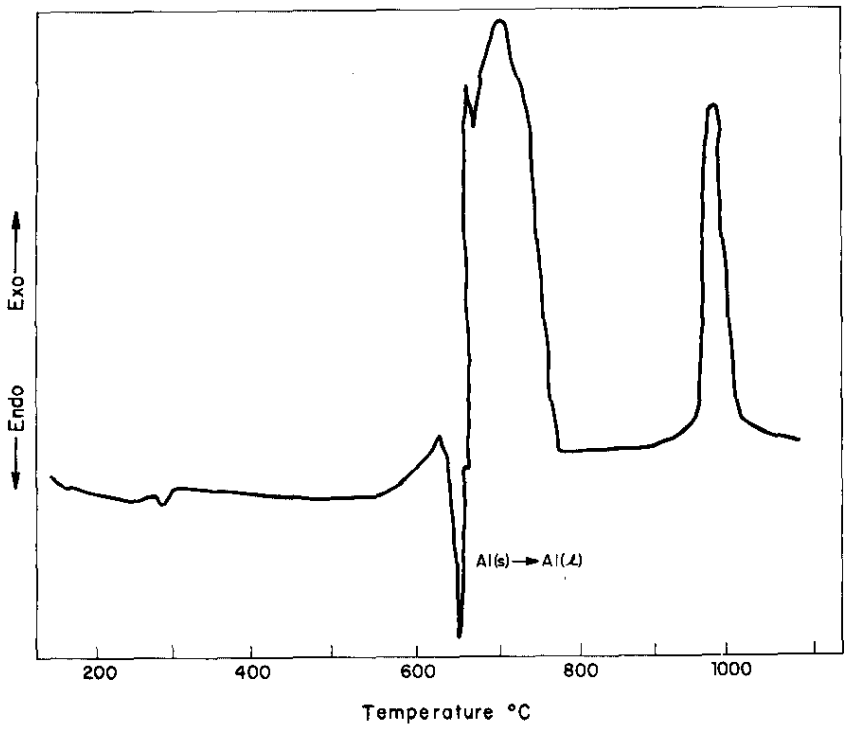


FIGURE 8. Typical DTA Curve for Group C-Al Compact

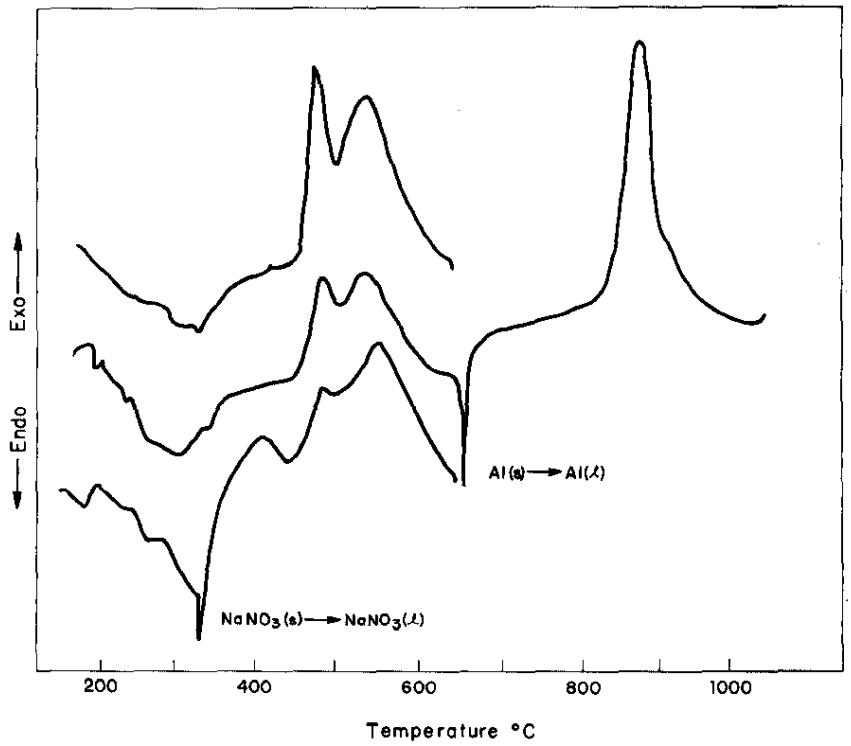


FIGURE 9. Typical DTA Curves for Group D-Al Compacts

TABLE 5

Estimated Energy Release from Exothermic Reactions of Each Group of Powders

| *Group* | *Temp. Range, °C* | *Estimated Release, Cal/g* |
|---|---|---|
| A | 600-660 | <10 |
| | >800 | 450 |
| B | 600-660 | <10 |
| | >800 | 500 |
| C | >600 | 2225 |
| D | 300-600 | 365 |
| | >800 | 2900 |

TABLE 6

Energy Available from Exothermic Reactions

| *Billet* | *Energy Release (kcal/billet) at Various Temp. Ranges* | | | |
|---|---|---|---|---|
| | *300-600°C* | *600-800°C* | *>800°C* | *Total* |
| 1001-1050[a] | - | - | 600 | 600 |
| 1051[a] | - | 2650 | 375 | 3025 |
| 1052[a] | - | 1775 | 450 | 2225 |
| 1053[a] | 15 | 6925 | 275 | 7215 |
| 1054[b] | 110 | 3675 | 225 | 4000 |
| 1055[b] | 110 | 4010 | 225 | 4250 |
| 1056[b] | 110 | 2375 | 350 | 2850 |
| 1057[b] | 100 | 2025 | 500 | 2625 |
| 1058[c] | 100 | 6025 | 125 | 6250 |
| 1059[c] | 110 | 6250 | 100 | 6450 |
| 1060[c] | 75 | 4675 | 250 | 5000 |
| 1061[c] | 100 | 4775 | 200 | 5075 |
| 1062[a] | 15 | 2350 | 700 | 3050 |
| 1063[a] | - | 450 | 825 | 1275 |
| 1064[a] | - | - | 700 | 700 |
| 1065[a] | - | 700 | 800 | 1500 |
| 1066-1074[a] | - | - | 600 | 600 |

*a.* These billets do not contain sufficient energy available for release below 600°C and therefore should not ignite the higher temperature reactions. No melting of the aluminum shells should be discernible.

*b.* These billets contain sufficient energy available for release below 600°C and sufficient total energy available for release to cause significant melting of the outer shell.

*c.* These billets contain sufficient energy available for release to melt all the aluminum in the shell.

## Visual Inspection of Reacted Billets

Identification numbers of five billets (1054, 1055, 1056, 1059, and 1061) were obliterated during the reaction in Furnace B. These billets were temporarily labeled A through E, and were subsequently identified by original number through thermal and chemical analyses. The cylindrical shapes of Billets B and E were lost completely. Portions of Billets A, C, and D remained as cylinders, with apparently unreacted core material in the remaining metal. Physical appearance indicated that one end of Billets C and D became much hotter than the other end. The physical damage to the billets from the heat released was visually ranked in the order B>E>C>D>A. Other billets in Furnace B showed evidences of internal reaction, but all remained intact and were readily identifiable.

The identification number of only one billet (1058) was obliterated in Furnace C. Billet No. 1060 showed massive melting but the end-ring with the identification number remained unmelted and identifiable. Other billets in Furnace C showed evidences of internal reaction, but all remained intact and readily identifiable.

## Sampling and Analysis of Reaction Residues

The seven billets (1054, 1055, 1056, 1058, 1059, 1060, 1061) which showed massive melting were divided into three sampling portions:

1) the top ash or slag (which was scraped from the billet residue and sampled before the residue was removed from the holding tray),

2) the apparently unreacted core material (which was physically removed),

3) the metallic mass (which was cut into pieces with an abrasive saw for sampling purposes).

At least three samples from each portion of the billets were analyzed by spark source mass spectrometry (SSMS), $^{252}Cf$ neutron activation, x-ray diffraction, and differential thermal analysis (DTA).

The ash samples were dissolved in aqueous solutions of HCl, $HNO_3$, $HNO_3$-KF, and $HNO_3$-KF-$Hg(NO_3)_2$. Dissolution was incomplete in each case. The principal constituents were determined to be $Al_2O_3$, $\alpha$-$U_3O_8$, $\beta$-$U_3O_8$, and $UO_2$. The apparently unreacted core material was determined to contain Al, $Al_2O_3$, $U_3O_8$, and $UO_2$.

The metallic mass was found to be aluminum and uranium-aluminides. The major impurities (100 to 500 ppm) were Fe, Ni, Zn, Si, and O. SSMS samples were too small to be homogeneous. Metallographic examination confirmed this microscale inhomogeneity. Even though the microdeterminations reveal the metallic mass to be an aluminum alloy containing a trace (0.7 to 6 wt %) of uranium, macrodeterminations showed ∿6% uranium; microregions varied from a trace to 20% U.

## Metallurgical Examination

Samples of the metallic mass were analyzed metallographically and tested for microhardness. Figure 10 shows a typical microstructure, which consists of eutectic and primary aluminide particles principally in boundaries between primary aluminum grains. The fairly large rounded grains indicate slow cooling after melting. Further evaluation of the microstructure is complicated by the expected large variation in uranium (0 to 20 wt %) within the billet. The presence of impurities and the possible gravity segregation of aluminide could result in large deviations from equilibrium microstructure. The diamond pyramid hardness (DPH) value of 35 in the primary aluminum grains is within error limits for a cast binary Al-U alloy (DPH 42), indicating very little alloying with elements other than aluminum.

## Billet Identification Determination

Analysis of the temperature charts of Furnaces B and C indicated that the billets reacted in sequence. Table 7 shows the internal energy release required to melt the total billet; less internal energy was required as the furnace temperature increased.

On the basis of the assumption that the average internal temperature at the beginning of reaction was 350 to 400°C for each billet and that loss of heat by radiation was insignificant, billets were identified (Table 8) by comparing the energy required for total melting (Table 7) with the energy available (Table 6).

Billets 1054, 1055, and 1056 contained some compacts that were mixtures of aluminum metal, $U_3O_8$, and $UO_3$, but contained no $NaNO_3$, $Na_2U_2O_7$, or $(NH_4)_3UO_2F_5$ as found in the more reactive billets. The absence of $UO_3$ in the residue of these three billets indicates an average temperature of less than 600°C where these less reactive compacts were grouped.

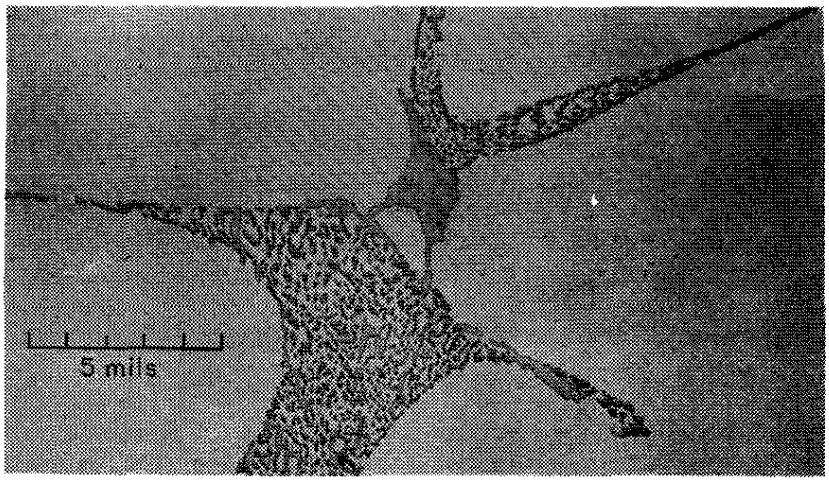


FIGURE 10. Microstructure of Reacted Al - Scrap Uranium Powders

TABLE 7

Internal Energy Required for Total Melting of a Billet

| *Temp., °C* | *Energy Required, kcal* |
|---|---|
| 350 | 5500 |
| 400 | 5150 |
| 450 | 4700 |
| 500 | 4300 |
| 550 | 3900 |
| 600 | 3500 |
| 660 | 2950 |

TABLE 8

Ranking of Billets by Extent of Reaction

| *Billet* | *Melting* | *Temporary Label* |
|---|---|---|
| 1059 | Complete | B |
| 1058 | Complete | - |
| 1061 | Almost Complete | E |
| 1060 | Almost Complete | - |
| 1054, 1055 | Partial | C, D |
| 1056 | Limited | A |

## DISCUSSION OF THERMOCHEMICAL DATA

### Group A Powders

DTA curves for Group A powders (Figure 3) are about the same as for pure $UO_3$. When compacted with aluminum powder, both Group A powders and $UO_3$ again show the same thermal events (Figure 6). The initial endotherm was the result of the loss of sorbed water. The second endotherm was the result of losing water of crystallization. The exotherm beginning at about 600°C* was the result of the following reactions:

(1) $3UO_3 = \alpha\text{-}U_3O_8 + \frac{1}{2}O_2$

(2) $3\ \alpha\text{-}U_3O_8(s) + 4Al(s) = 2Al_2O_3(s) + 9UO_2(s)$

(3) $3UO_3 + 2Al(s) = Al_2O_3(s) + 3UO_2(s)$

These reactions occurred only at the particle boundaries and were quenched when the aluminum melted at 660°C as shown by the endothermic peak. The exothermic peak beginning at about 900°C was the result of the following set of possible reactions:

(4) $3U_3O_8(s) + 4Al(\ell) = 2Al_2O_3(s) + 9UO_2(s)$

(5) $3U_3O_8(s) + 16Al(\ell) = 8Al_2O_3(s) + 9U(\ell)$

(6) $3U_3O_8 + 34Al(\ell) = 8Al_2O_3(s) + 9UAl_2(\ell)$

(7) $3U_3O_8(s) + 43Al(\ell) = 8Al_2O_3(s) + 9UAl_3(\ell)$

(8) $3U_3O_8(s) + 52Al(\ell) = 8Al_2O_3(s) + 9UAl_4(\ell)$

(9) $3UO_2(s) + 4Al(\ell) = 2Al_2O_3(s) + U(\ell)$ [or $UAl_2(\ell)$, $UAl_3(\ell)$, $UAl_4(\ell)$]

Only $UO_2$, $Al_2O_3$, and primary uranium aluminides have been identified in the reaction products. Cooling curves for the product indicated the presence of $UAl_4$ (the available temperature range was insufficient to detect the presence of U, $UAl_2$, or $UAl_3$).

---

* Further work by P. E. Doherty, SRL, has shown that at least part of the 600°C exotherm may be due to the reaction of sorbed oxygen with the aluminum metal.

The reduction of the impurities $Fe_2O_3$ and $Cr_2O_3$ by aluminum, i.e., the typical "thermite" type reactions,[11] are ignited around 1000°C. These reactions, however, supplied only a very minor amount of energy to meltdown incident.

In typical DTA curves for the residues of the Group A powders - aluminum reactions (Figure 11), only the alloy melting endotherm and solidification exotherm were found.

## Group B Powders

DTA curves for Group B powders (Figure 3) are about the same as those for pure $UO_3$. When compacted with aluminum powder, both Group B powders and $U_3O_8$ again show the same thermal events (Figure 7). The first and second exotherms are the result of losing water. The exotherm beginning at about 600°C was the result of Reaction 2 above. This reaction occurred only at the particle boundaries and was quenched when the aluminum melted at 660°C, as shown by the endothermic peak. The exothermic peak beginning at about 700°C was the result of Reactions 4 through 8 above.

Typical DTA curves for the residues of the Group B powders - aluminum reactions are shown in Figure 11; only the alloy melting endotherm and solidification exotherm were found.

The exothermic reactions between aluminum and $U_3O_8$ have been studied by Fleming and Johnson;[12] Handwerk, et al.;[13] Gibson and Shupe;[14] and by Vogel, et al.[15] The findings here are in agreement with the findings of Fleming[12] and Handwerk.[13] Other published data[14,15] suggest that $UAl_4$ is also formed during the reaction at about 600°C. However, we found x-ray diffraction evidence for $UO_2$, but not for $UAl_4$.

## Group C Powders

Typical DTA curves for Group C powders are shown in Figure 4. The first endotherm was from loss of water. The second endotherm was due to the decomposition of the $(UH_4)_3UO_2F_5$ in the mixture. If this material had been calcined at a temperature of 700°C, only $U_3O_8$, $AlF_3$, and $Al_2O_3$ would have been found in the mixture.

In typical DTA curves for the Group C powders - aluminum compacts (Figure 8), the large exothermic peak occurring near the melting point of aluminum was due to the following set of possible reactions:

(10) $(NH_4)_3UO_2F_5(s) \rightarrow UO_2F_2(s) + 3NH_4F(s)$

(11) $2Al(\ell) + 3UO_2F_2(s) \rightarrow 2AlF_3(s) + 3UO_2(s)$

(12) $NH_4F(s) \rightarrow NH_3(g) + HF(g)$

(13) $6HF(g) + 2Al(\ell) \rightarrow Al_4F_3(s) + 3H_2(g)$

(14) $4Al(\ell) + 3UO_2(s) \rightarrow 2Al_2O_3(s) + U(\ell)$

(15) $6Al(\ell) + 3UO_2(s) \rightarrow 2Al_2O_3(s) + Al_2U(\ell)$

(16) $7Al(\ell) + 3UO_2(s) \rightarrow 2Al_2O_3(s) + Al_3U(\ell)$

(17) $8Al(\ell) + 3UO_2(s) \rightarrow 2Al_2O_3(s) + Al_4U(\ell)$

Typical DTA curves for the residues of the Group C powders - aluminum reaction residues, are shown in Figure 11. Only the alloy-melting endotherm and solidification exotherm were found.

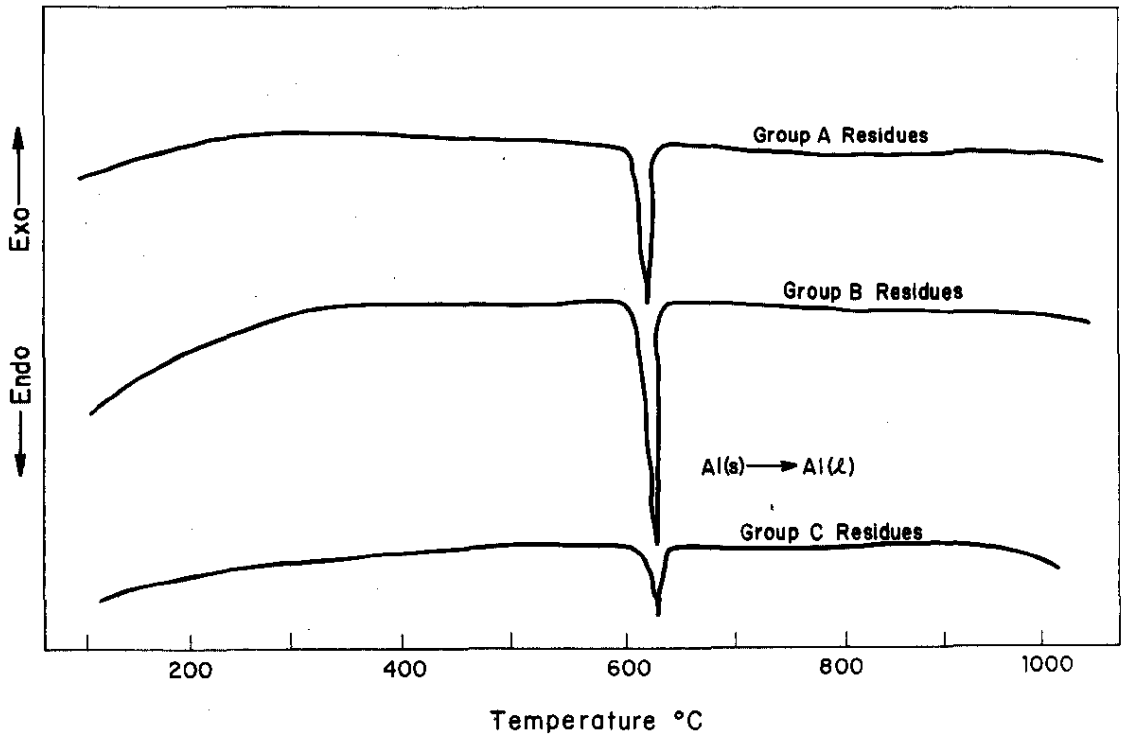


FIGURE 11. Typical DTA Curves for Groups A, B, and C - Al Compact Reaction Residues

## Group D Powders

Typical DTA curves for Group D Powders are shown in Figure 5. The first group of endotherms was a result of water loss. The second group of endotherms reflects the decomposition of sodium nitrate. After this material was cycled several times from ambient to about 450°C, the $NaNO_3(s) \rightarrow NaNO_3(\ell)$ transition at 310°C was also observed. The non-homogeneity of these samples was shown by the differences in area under the endothermic peaks.

A typical DTA curve for $Na_2U_2O_7$ is shown in Figure 12, Curve A; thermal events were noted. However, when heated in the high temperature x-ray diffraction camera, $Na_2U_2O_7$ exhibited two reversible phase changes at 365°C and 1075°C, which were verified by observing small changes in the x-ray pattern. In complete agreement with Cordfunke and Loopstra,[16] our DTA and TGA experiments showed that $Na_2U_2O_7$ is thermally stable to at least 1200°C.

When $Na_2U_2O_7$ was compacted with aluminum powder, three exothermic reactions were observed (Curve B). The first reaction began at about 225°C. X-ray diffraction and electron-probe analysis of compacts (which had been held at 360°C for about 16 hours) showed this solid state reaction occurred only at the particle interfaces. Typical microstructures of unreacted and reacted pellets are shown in Figure 13. The unreacted pellet contained large round grains of silvery aluminum and orange $Na_2U_2O_7$. The reacted pellet contained silvery grains and black particles with very irregular edges. When the reacted pellet was broken and a differential thermogram run, the reaction went to completion (Figure 12, Curve C). However, when the reacted pellet was ground and recompacted before obtaining a differential thermogram, additional exothermic reaction occurred. X-ray diffraction of the ground pellets showed the major constituents to be the starting materials: aluminum and $Na_2U_2O_7$. From this, we concluded that the reaction was a surface reaction only. For verification, the profiles of aluminum and uranium concentrations were obtained with the electron microprobe. The profiles were obtained by starting the scan in an aluminum grain, traversing the particle interface, through a $Na_2U_2O_7$ particle, across the opposite interface, and into a second aluminum grain. Figure 14 shows these scans. In the unreacted pellet, the concentration profile shows very sharp boundaries between aluminum and uranium. In the reacted pellets, however, there is a layer containing both aluminum and uranium at the interface. Although verifying experiments were not made, the solid state reduction of the uranium oxides is assumed to occur at the particle interfaces since the reactions as well as x-ray data are similar.

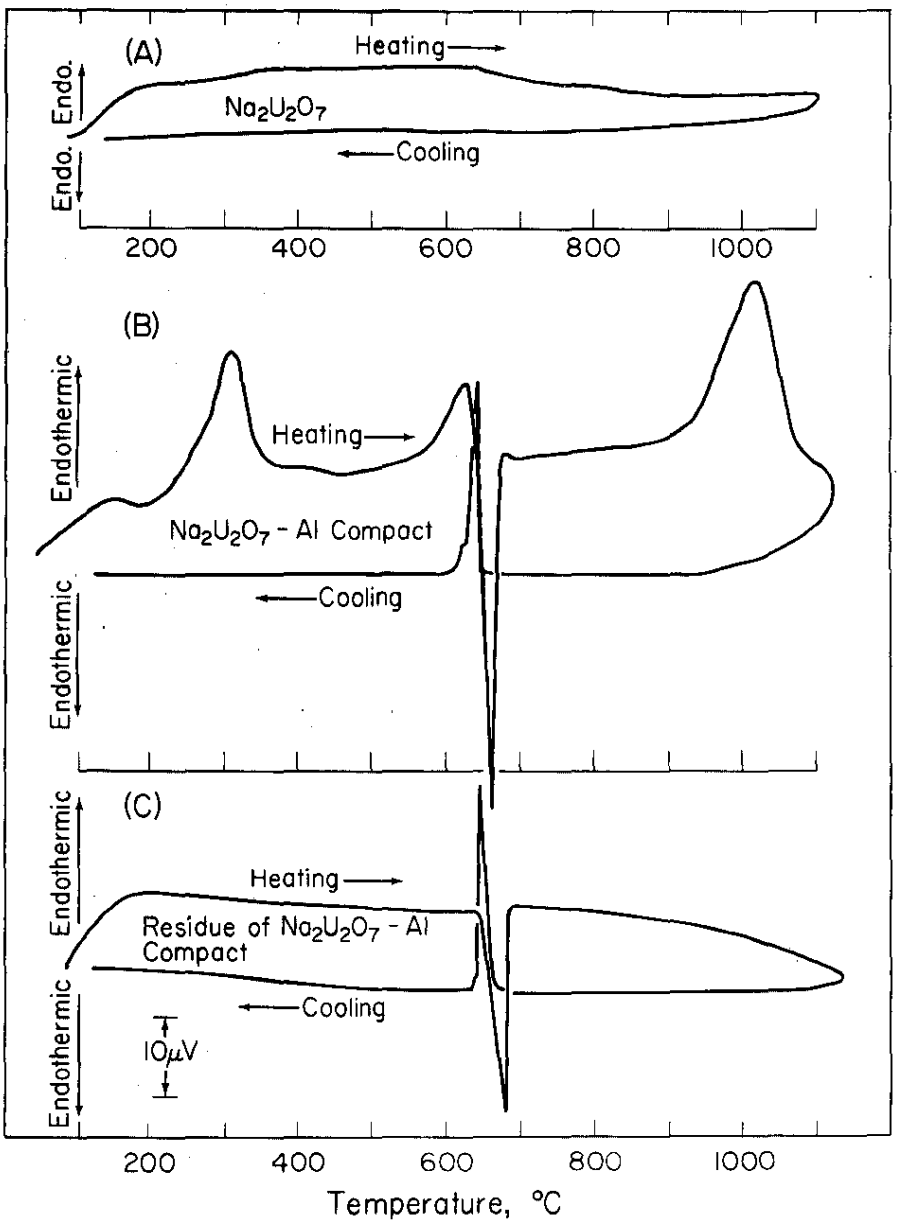


FIGURE 12. DTA Curves for $Na_2U_2O_7$, $Na_2U_2O_7$-Al Compact, and Reaction Residue

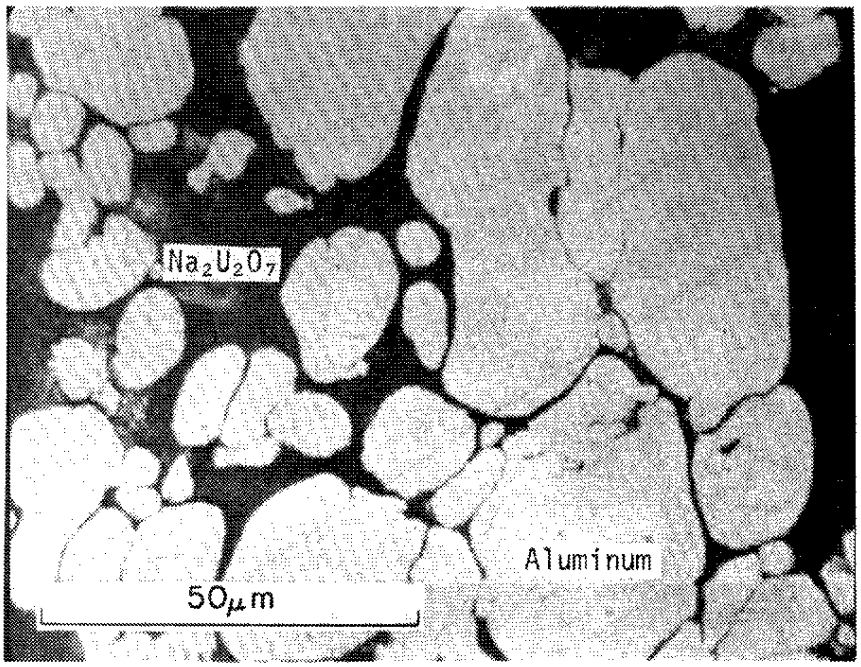


a. Unreacted (as-pressed)

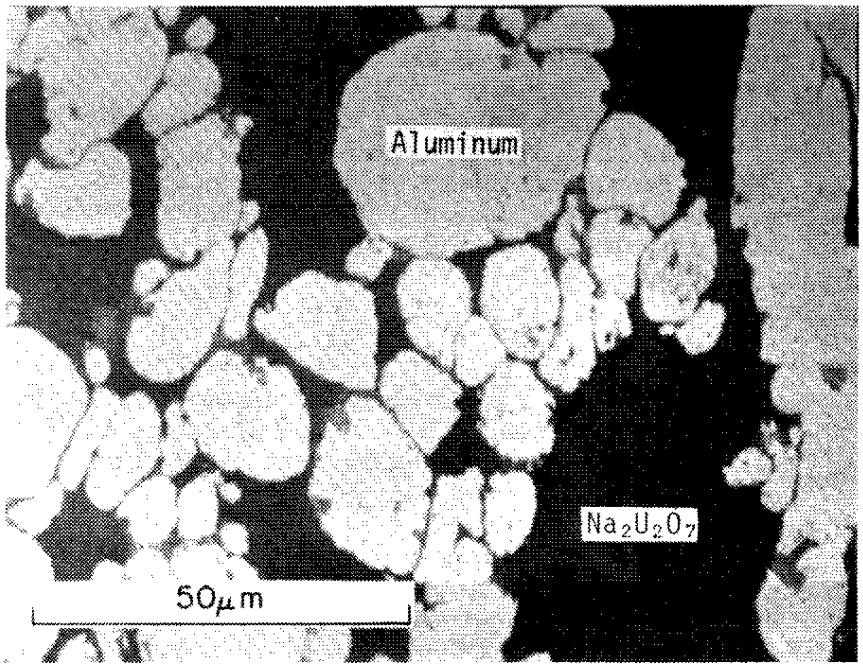


b. Reacted (heated 16 hr at 360°C)

FIGURE 13. Microstructures of Al-$Na_2U_2O_7$ Pellets

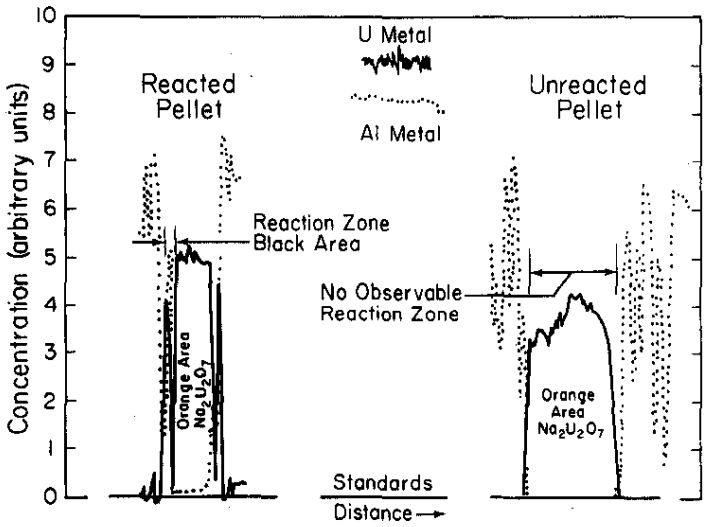


FIGURE 14. Electron Microprobe Scan of Al-$Na_2U_2O_7$ Pellets Showing the Interfacial Reaction Zone

Typical DTA curves for the aluminum compacts of Group D powders are shown in Figure 9. When compared to Figure 5, several changes have occurred. The endothermic loss of water has evidently been modified, as the diffusion of water from the compacted powders was much slower than from the loose powder. Some ions redistributed upon compacting as shown by the sharp melting endotherm for sodium nitrate. Differences in the calcination time or temperature between batches of Group D material is indicated by the change in the ratio of the areas under the first and second exothermic peaks of the aluminum compacts. The area under the first exothermic peak is proportional to the amount of $Na_6U_7O_{24}$ present in the sample; the area under the second peak is proportional to the amount of $Na_2U_2O_7$ present in the sample.

When the uranate was precipitated from aqueous solution, washed free of the excess sodium nitrate, air-dried, compacted with aluminum, and subjected to DTA, Curve A in Figure 15 resulted. X-ray lines for $Na_6U_7O_{24}$ were very pronounced in this sample. Curve B obtained with commercially prepared $Na_2U_2O_7$ showed much less pronounced x-ray lines for $Na_6U_7O_{24}$. Curve C was obtained with $Na_2U_2O_7$ prepared according to the method of Cordfunke and Loopstra,[16] followed by heating one week. X-ray lines for $Na_6U_7O_{24}$ were not observed in this sample.

As the amount of $Na_6U_7O_{24}$ decreased, the first peak of the initial exothermic doublet (Figure 15) decreased and the second peak increased. X-ray diffraction and electron-probe analysis of compacts of $Na_2U_2O_7$ which had been held at 360°C for varying periods of time showed this solid-state reaction occurred only at the particle boundaries.[17]

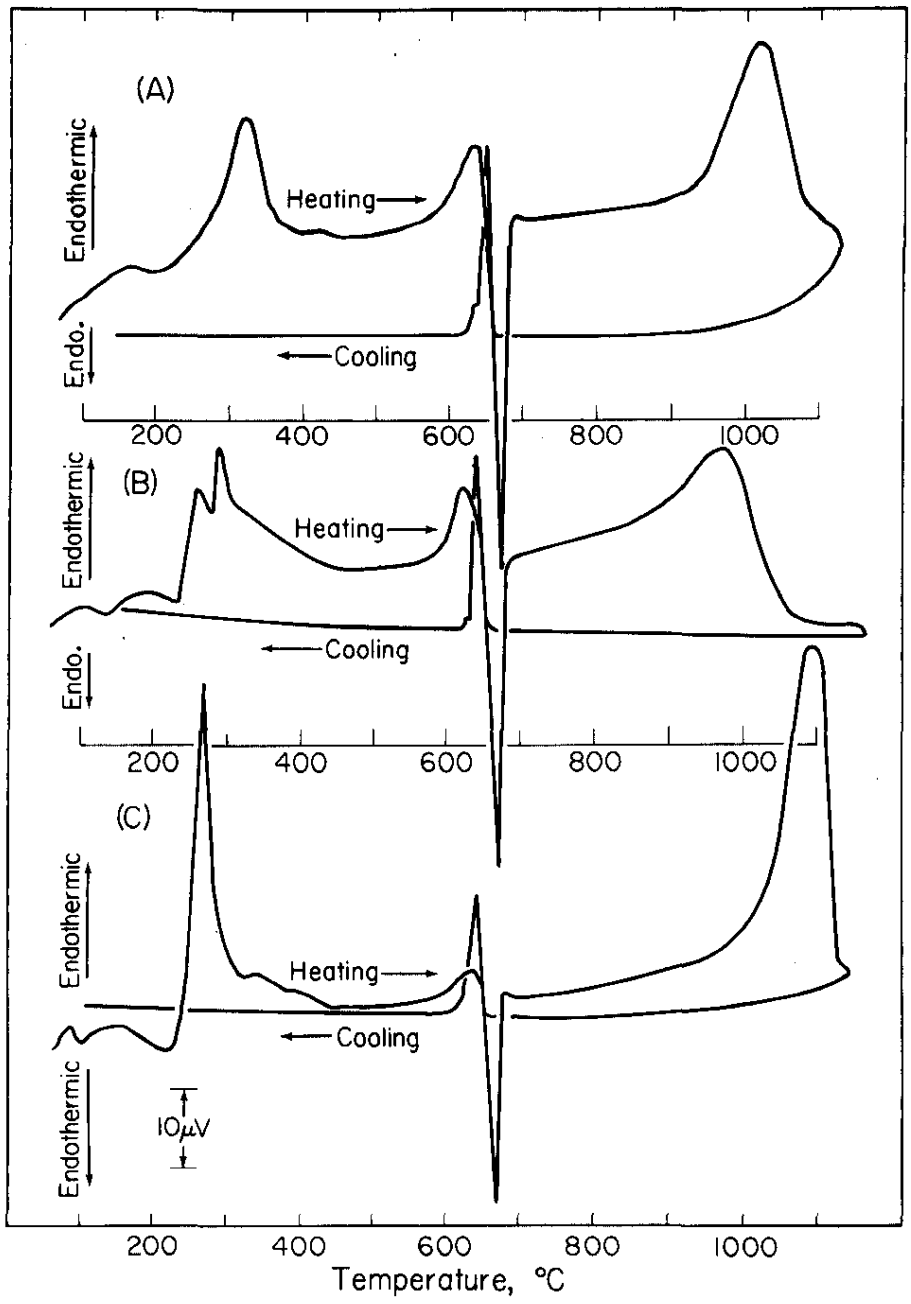


FIGURE 15. DTA Curves of Mixtures of $Na_2U_2O_7$-$Na_6U_7O_{24}$-Al in Pressed Compacts

The second exothermic reaction began at approximately 600°C. The area under the peak was dependent upon how long the compact had been held at about 350°C. When heated at 30°C per minute, the Group D powders exhibited little or no exotherm in this region. However, if held at about 350°C for a few hours, and then heated at 30°C per minute, a small exotherm was evident. All of the clean preparations of sodium uranate exhibit this exotherm when heated at 30°C per minute (Figure 15). The area under the curve, however, increased when the compact was held at 350°C for several hours before running the DTA. This increase indicated the possible solid-state reactions at about 350°C were

(18) $9Na_2U_2O_7(s) + 4Al(s) \rightarrow 9Na_2O(s) + 2Al_2O_3(s) + 6U_3O_8$

(19) $9Na_4U_7O_{24} + 14Al \rightarrow 27Na_2O(s) + 7Al_2O_3(s) + 21U_3O_8$

The second exothermic reaction, then, is the same as Reaction (2) above. This reduction of uranium to $UO_2$ is quenched when the aluminum melts (endotherm at 660°C).

The third exothermic event between Group D material and aluminum was the result of two reactions:

1. The oxidation of aluminum by sodium nitrate,[18] (Figure 16).

2. The complete reduction of the uranium compounds to the U-Al alloy.

The reaction between aluminum and sodiun nitrate was not studied in detail. However, the expected products are $Al_2O_3$, $Na_2O$, nitrogen oxides, and possibly nitrogen gas.

The following set of reactions is proposed to account for the reduction of the uranates at about 900°C:

(20) $Na_2U_2O_7(s) + 2Al(\ell) \rightarrow Na_2O(s) + Al_2O_3(s) + U$

(21) $Na_2U_2O_7(s) + 4Al(\ell) \rightarrow Na_2O(s) + Al_2O_3(s) + UAl_2$

(22) $Na_2U_2O_7(s) + 5Al(\ell) \rightarrow Na_2O(s) + Al_2O_3(s) + UAl_3$

(23) $Na_2U_2O_7(s) + 6Al(\ell) \rightarrow Na_2O(s) + Al_2O_3(s) + UAl_4$

(24) $Na_6U_7O_{24}(s) + 14Al \rightarrow 3Na_2O + 7Al_2O_3 + 7U$

(25) $Na_6U_7O_{24}(s) + 21Al \rightarrow 3Na_2O + 7Al_2O_3 + 7UAl_2$

(26) $Na_6U_7O_{24}(s) + 28Al \rightarrow 3Na_2O + 7Al_2O_3 + 7UAl_3$

(27) $Na_6U_7O_{24}(s) + 35Al \rightarrow 3Na_2O + 7Al_2O_3 + 7UAl_4$

(28) $2Na_2O(s) \xrightarrow{>1100°C} 4Na(g) + O_2(g)$

At the Al-to-U ratio used, the most predominant aluminides precipitated would be $UAl_3$ and $UAl_4$.

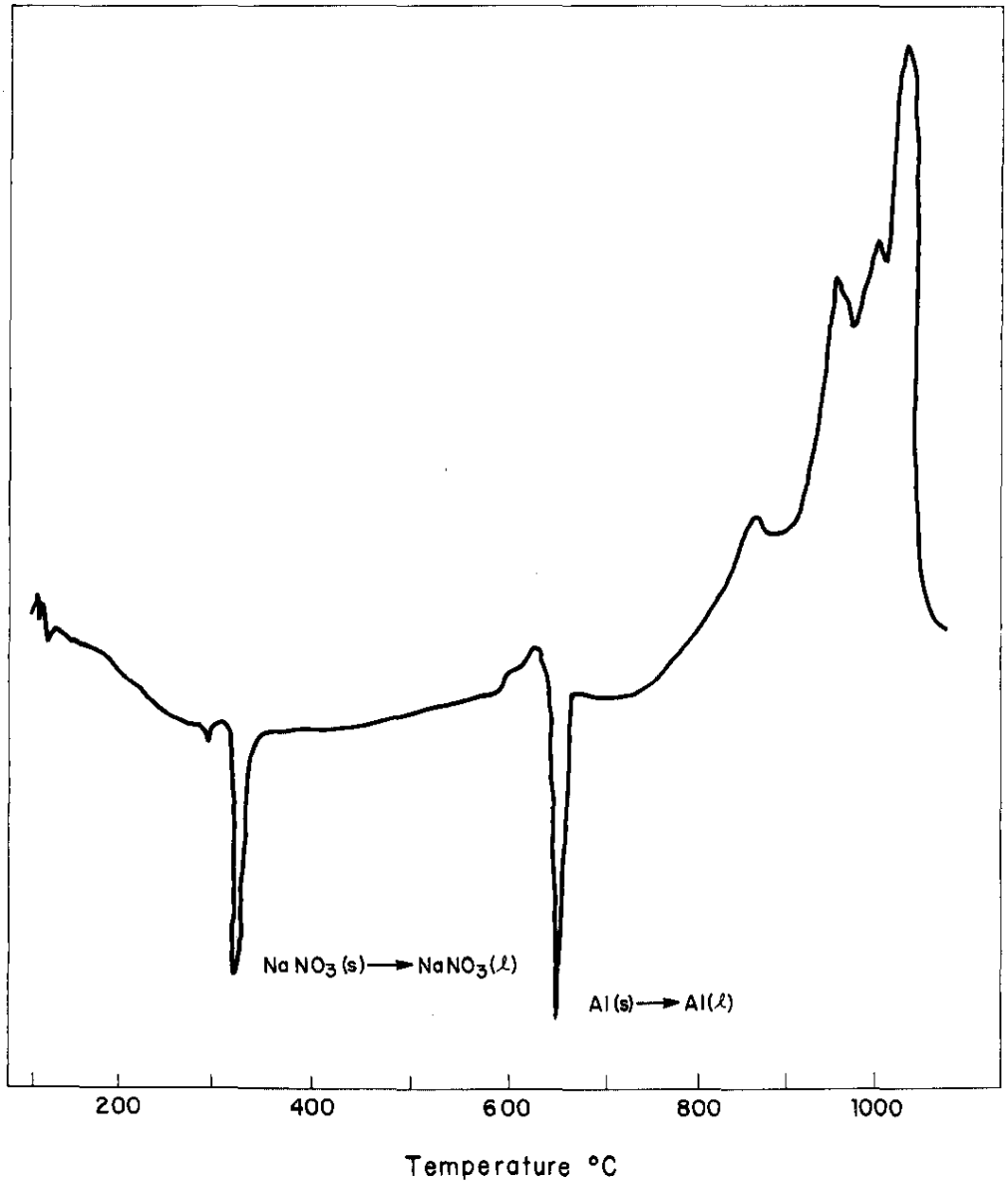


FIGURE 16. Typical DTA Curve for $NaNO_3$-Al Reaction

## Reaction Sequence

The initial reaction in each billet was between Al(s) and the mixed uranate salts in Group D. Eight billets (1054 through 1061) contained compacts in which 50% or more of the scrap oxide content was Group D material. Thermodynamic calculations show that if the high temperature oxidants $Na_2U_2O_7(s)$ and $Na_6U_7O_{24}(s)$ were mixed homogeneously, none of the higher temperature reactions would ignite. However, homogeneous mixing requires that the aluminum oxide and scrap powders be matched closely in particle size. Because particle size matching was not attempted in the preparation of the billets, local concentrations of $Na_2U_2O_7$ may have been excessive. In Billets 1059, 1060, and 1061, a 30% local excess of $Na_2U_2O_7$ would have provided more energy than needed to raise local temperature from 350 to 650°C, and thus initiate the higher energy reactions.

The most energetic reactions such as that between Al(ℓ) and $NaNO_3(\ell)$ ignite between ∿620°C and 800°C. The products of this reaction are a mixture of nitrogen, sodium, and aluminum oxides. The second set of important reactions is between Group C powders and Al(ℓ). These two sets of reactions account for ∿92% of the energy released in the furnaces.

The reactions above 800°C are between Al(ℓ) and metal oxides such as $U_3O_8$, $Fe_2O_3$, $Cr_2O_3$, $Co_3O_4$, and NiO. Published data[11,18-20] are sufficient to calculate the available energy. These reactions account for only ∿5% of the total energy released in the furnaces.

## RECOVERY OF THE $^{235}U$

The data revealed that reactive compounds were not blended into 28 (1033-1050, 1064, and 1066-1074) of the 42 billets that were stored following the meltdown incident. The uranium in 27 of these 28 billets was recovered by extrusion into tubes followed by dissolution as originally envisioned. The remaining billet (1066, containing only $U_3O_8$-Al compacts) had become contaminated either during the incident or during storage and handling, and could not be sufficiently decontaminated for the extrusion process.

The uranium in the residue of 4 of the billets was recovered by reducing the uranium compounds with an aluminum-lithium fluoride flux and casting the resulting U-Al alloy into cylindrical ingots. These ingots will be dissolved and the uranium purified by the normal solvent extraction techniques. Processing was discontinued to permit modifying the building to install equipment for another glove box line. The remaining 11 billets are stored and will be processed at a later time.

## REFERENCES


1. J. S. Hirschorn. *Introduction to Powder Metallurgy*, American Powder Metallurgy Institute, New York (1969).
2. H. H. Hausner. *Powder Metallurgy in Nuclear Engineering*, American Society for Metals, Cleveland (1958).
3. S. D. Smiley, J. W. Langhaar, and R. Maher. *Chem. Eng. Prog. Symp. Series, 60*, 65 (1964).
4. P. M. Kranzlein. *Corrosion of Stainless Steel in $HNO_3$-HF Solutions*, USAEC Report DP-486, E. I. du Pont de Nemours and Co., Savannah River Laboratory, Aiken, S.C. (1960).
5. T. H. Siddall, III. "Solvent Extraction Processes Based on Tri-n-butyl Phosphate," Chapter V in *Chemical Processing of Reactor Fuels*, Academic Press, New York (1961).
6. F. N. Culler, Jr. and F. R. Bruce. *Proc. 1st Intern. Conf. Peaceful Uses Atomic Energy, Geneva, 1955*, p. 541 (1956).
7. D. G. Karraker. *Proc. 2nd Intern. Conf. Peaceful Uses Atomic Energy, Geneva, 1958*, p. 519 (1958).
8. C. Buck, G. R. Howells, T. A. Parry, B. F. Warner, and J. A. Williams. *Proc. 2nd Intern. Conf. Peaceful Uses Atomic Energy, Geneva, 1958*, p. 82 (1968).
9. R. J. Christl and A. E. Daking. *Chem. Eng. Prog. Symp. Series, 60*, 1 (1964).
10. A. W. Joyce, Jr., L. C. Peery, and E. B. Sheldon. *Chem. Eng. Prog. Symp. Series, 56*, 21 (1960).
11. L. Graffing. *Welding Handbook*, A. L. Phillips (ed.) 6th ed., Vol. 3B, p. 57.4, American Welding Society, New York (1971).
12. J. D. Fleming and J. W. Johnson. *Research Reactor Fuel Element Conference, September 17-19, 1962, Gatlinburg, Tennessee.* U.S. Government Report TID-7642, p. 649f, Oak Ridge, Tennessee (1962).
13. J. H. Handwerk, R. A. Noland, and D. E. Walker. *Uranium-Oxide-Containing Fuel Element Composition and Method of Making Same.* U.S. Patent No. 2,805,473 (1957).
14. G. W. Gibson and O. K. Shupe. *Annual Progress Report on Fuel Element Development for Fiscal Year 1961.* USAEC Report IDO-16727, Phillips Petroleum Co., Arco, Idaho (1962).

15. R. C. Vogel, M. Levenson, and V. H. Minnecke. *Chemical Engineering Division Semi-Annual Report, July-December, 1963.* USAEC Report ANL-6800, Argonne National Laboratory, Argonne, Illinois (1964).

16. E.H.P. Cordfunke and B. O. Loopstra. "Sodium Uranates." *J. Inorg. Nucl. Chem., 33,* 2427 (1971).

17. L. W. Gray and W. J. Kerrigan. "A DTA, TGA, and Metallurgical Study of the Exothermic Reactions Between Aluminum and Uranium Compounds." *J. Inorg. Nucl. Chem. 38,* 1641 (1976).

18. K. P. Zakharova, et al. *Soviet At. Energy, 24,* 475 (1968); *CA 69,* 29986m, "Use of Chemical Reaction Heat for Thermal Treatment of Radioactive Wastes."

19. O. Kubaschewski, et al. *Metallurgical Thermochemistry,* 4th ed., p. 244, Pergamon Press, New York (1967).

20. R. C. Weast (ed.). *Handbook of Chemistry and Physics,* 49th ed., p. D-33, The Chemical Rubber Co., Cleveland, Ohio (1968).